의학석사학위논문

Magnetic Resonance Imaging Findings of Spinal Arteriovenous Fistulas

−Focusing on Localization of Fistulas and Differentiation between Spinal Dural and Perimedullary Arteriovenous Fistulas−

척추동정맥루의 자기공명영상 소견

–동정맥루의 위치 결정과 경막동정맥루와 척추주위동정맥루 간 감별–

2016년 2월

서울대학교 대학원

의과대학 임상의과학과

양현경

Abstract

Magnetic Resonance Imaging Findings of Spinal Arteriovenous Fistulas

−Focusing on Localization of Fistulas and Differentiation between Spinal Dural and Perimedullary Arteriovenous Fistulas−

Hyun Kyung Yang

Department of Clinical Medical Sciences

The Graduate School

Seoul National University

***Purpose*:** To investigate the MRI findings of spinal arteriovenous fistulas (AVFs) to predict their locations and types.

***Materials and Methods*:** Patients who underwent spinal angiography for suspected spinal AVF between April 2003 and April 2013 were enrolled. Spine MRIs were analyzed by two radiologists in consensus focusing on the distribution patterns of flow void pial vessels (FVPVs): longitudinal

distribution pattern along the spinal level (even or uneven, with description of the most crowded level in uneven cases) and axial distribution pattern in relation to the cord (ventral, dorsal or co-dominance). Spinal angiography served as the reference standard for the locations and types of fistulas.

***Results*:** Thirty two patients (M:F=24:8, mean age, 53 years; range, 2–74 years) were included. There were 18 patients with spinal dural AVFs (SDAVFs), seven with perimedullary AVFs, four with epidural AVFs, and three diagnosed as normal. In 12 of 15 longitudinally uneven AVFs, the most crowded levels of FVPVs ± ≤two-level corresponded to the true fistulous level. While dorsal dominance was predominant in SDAVFs (13/18), ventral dominance was major in perimedullary AVFs (5/7) ($P < 0.01$).

***Conclusion*:** Fistulous levels may be predicted to be within the most crowded level of FVPVs ± two-level. The dorsal dominance pattern of FVPVs favors SDAVFs while the ventral dominance pattern suggests perimedullary type.

Keywords: Central Nervous System Vascular Malformations; Spinal Cord Diseases; Arteriovenous Fistula; Magnetic Resonance Imaging; Angiography

Student number: 2014-22212

Contents

List of Tables

List of Figures

Introduction

Vascular malformations of the spinal cord are classified into types according to their location and vascular pathology (1, 2) and show wide morphological variation. Among them, spinal dural arteriovenous fistulas (SDAVFs) and perimedullary arteriovenous fistulas (AVFs) are fistulas without nidus. SDAVFs consist of a vascular shunt located in the dura along the spinal canal near the neural foramen region. The arterial supply commonly arises from a dural branch of the radicular artery, with the draining vein piercing the dura several millimeters from the accompanying nerve root (either above or below it) to reach the engorged perimedullary veins (coronal venous plexus) (3-6). On the other hand, perimedullary AVFs are direct arteriovenous shunts located superficially on the spinal cord and only rarely possess intramedullary compartments (7). Feeding vessels can be either the anterior or posterolateral spinal artery, while the draining veins are superficial perimedullary veins.

Findings of spinal AVFs at conventional spin-echo MRI include central hyperintensity on T2-weighted images within the lower spinal cord and conus medullaris, gadolinium enhancement within the cord, and multiple vascular flow voids along the surface of the cord (3-5); however, these findings are of minimal assistance in the characterization and localization of a malformation. Therefore, the value of a multidetector computed tomographic angiography (MDCTA) and contrast-enhanced MR angiography (CEMRA) in predicting the fistulous level has been studied (8-15) to help planning and reducing angiography. On the other hand, to our knowledge there has been no report on the localization of fistulas and differentiation of fistulous type with conventional MRI findings. Hence, the purpose of this study was to

investigate MRI findings of spinal AVFs, focusing on the localization of fistulous level and differentiation of AVF type.

Materials and Methods

Patients

This retrospective study was approved by the institutional review board and the requirement for informed consent was waived. Patients who underwent spinal angiography for suspected spinal AVF between April 2003 and April 2013 were enrolled. The suspicion of spinal AVF was made by radiologists based on the spine MRI findings or a neurosurgeon based on the clinical symptom. Inclusion criteria were patients who 1) underwent spinal angiography in our institute due to suspicion of spinal vascular malformation, 2) had records describing spinal angiography findings, and 3) underwent spine MRI before angiography. Exclusion criteria were patients who 1) underwent spinal angiography for preoperative embolization of a hypervascular spinal tumor, 2) did not undergo spine MRI before angiography. One radiologist with 5 years of experience retrospectively reviewed the medical records to investigate the symptom (motor, sensory, or sphincter dysfunction), mode of onset (acute or insidious; onset within the past 2 weeks was defined as acute and otherwise as insidious), duration of symptom, and treatment response (good, fair, or poor).

MRI protocol

Spine MRIs were performed on either a 1.5T unit (Gyroscan Intera; Philips Healthcare, Best, the Netherlands) or a 3.0T unit (Achieva; Philips Healthcare) by using a receive-only synergy spine coil in our institute. Each study consisted of axial (TR/TE, 572–631/9–20 msec) and sagittal T1-weighted (TR/TE, 453–600/10–17 msec) and T2-weighted (axial, TR/TE, 4500–6364/120 msec; sagittal, TR/TE, 3500–3674/120 msec) images with a

field of view of 150–160 × 150–160 mm for the axial and 260–350 × 260–350 mm for the sagittal images. Section thickness was 3, 4, or 8 mm with a 10%, 20%, or 25% intersection gap. The echo-train lengths were 3–9 for the T1-weighted images and 15–30 for the T2-weighted images. A 188–216 × 188–216 matrix was used for the axial images and a 280–512 × 280–512 matrix for the sagittal images. Contrast-enhanced T1-weighted MRIs after intravenous injection of gadopentetate dimeglumine (0.1 mmol/kg, Magnevist; Schering, Berlin, Germany) were performed in 18 of 19 cases.

Among the patients who underwent spine MRI elsewhere with various scanners and various MR parameters, only those who had both sagittal and axial T2-weighted images were included in this study.

Spinal angiography

Spinal angiography was performed via a femoral approach in a dedicated biplanar neuroangiographic suite (Integris BN V3000; Phillips Healthcare) by either a neurosurgeon or a neuroradiologist. Standardized angiography included selective manual injections of 4–5 mL of 300 mg/mL of iodinated nonionic contrast medium into lumbar and intercostal arteries to find AVFs. If an AVF was failed to be demonstrated on the standardized angiography or the fistula was located close to any of the following arteries, injections into both vertebral arteries, the costocervical arteries, the thyrocervical trunks, and the iliolumbar arteries were added. Imaging was in the anteroposterior direction with 2 frames per sec. Film sequences of at least 5–20 seconds were taken, depending on the underlying vascular pathology, to evaluate the venous drainage. In all cases, the angiography included identification of all the arteries supplying the thoracolumbar cord.

MRI analysis

The spine MRIs were retrospectively evaluated by two radiologists (15 and 5 years of experience in spinal radiology, respectively) who were blinded to the clinical and angiographic findings, in consensus. They assessed the following MRI findings: (a) longitudinal distribution pattern of multiple engorged flow void pial vessels (FVPVs) along the surface of the cord (a nominal variable categorized as even or uneven; in uneven cases, the most crowded level of the FVPVs was described), (b) axial distribution pattern of FVPVs in relation to the cord (a nominal variable categorized as ventral dominance, dorsal dominance, or codominance), (c) longitudinal extent of T2 high signal intensity (SI) in the cord (a continuous variable counted as the number of vertebral segments), and (d) presence of contrast enhancement in the cord (a nominal variable categorized as present or absent). The longitudinal distribution pattern of FVPVs referred as to whether a particular part of FVPVs could be identified as more crowded than the others along the spinal level(s), and the axial distribution pattern represented as to whether FVPVs were dominantly noted either in the ventral, dorsal or both side(s) of the cord.

Comparison of MRI findings with spinal angiography findings

In the group of uneven longitudinal FVPVs, the most crowded level of FVPV on spinal MRI was compared with the true fistulous level confirmed on spinal angiography and categorized as follows: equal, ± one-level difference, ± two-level difference, or ± three-level or more difference. In the other population with even longitudinal FVPVs, we investigated which part the true fistulous level had belonged to among the followings: more cranial to the

highest FVPV, cranial 1/3 within FVPVs, middle 1/3 within FVPVs, caudal 1/3 within FVPVs, or more caudal to the lowest FVPV.

The axial distribution pattern of the FVPV on the cord pial surface was related to the type of AVF. The presence of a T2 high SI and contrast enhancement in the spinal cord was compared with the duration of myelopathy.

Statistical analysis

To focus on the study objectives, only data of SDAVFs and perimedullary AVFs were used and those of epidural AVFs and normal were excluded in the statistical analysis. Mean values for patients' sex, age, and duration of myelopathy between SDAVF (n = 18) and perimedullary AVF (n = 7) groups were compared using Fisher's exact test for the categorical variable (sex) and the Mann-Whitney test for continuous variables (age and duration of myelopathy), respectively. To find out if there is significant difference in the longitudinal and axial distribution patterns of FVPVs between SDAVFs and perimedullary AVFs, Fisher's exact test was used. The relationship between the longitudinal extent of the T2 high SI in the spinal cord and the duration of myelopathy was evaluated by Spearman correlation analysis. To analyze if there is significant difference in the duration of myelopathy between the groups with and without T2 high SI in the cord, and between those with and without contrast enhancement in the cord, Mann-Whitney test was used. Since contrast enhancement studies were not performed in five cases, we excluded them when performing the aforementioned analysis. All statistical analyses were conducted using SPSS 16.0.1 software (SPSS, Chicago, Ill). $P < 0.05$ indicated statistical significance.

Results

Thirty two patients (24 men and eight women) were included in this study. The mean age was 53 years (range, 2–74 years). Nineteen of the 32 patients underwent spine MRI in our institute, and 13 patients underwent spine MRI in other hospitals. The interval between MRI and spinal angiography ranged from 1 to 4 days. There were 18 patients with SDAVFs, seven with perimedullary AVFs, three with epidural AVFs associated with chronic vertebral fractures, one with an epidural AVF associated with an acute vertebral fracture, and three diagnosed as normal based on spinal angiographies. Demographics and clinical findings of each group are summarized in Table 1. MRI findings of SDAVFs and perimedullary AVFs are summarized in Tables 2 and 3.

There was a significant difference in patients' age between SDAVFs (mean age, 59 years) and perimedullary AVFs (mean age, 39 years) ($P = 0.012$) (Table 1). Demographics of 18 SDAVF and seven perimedullary AVF patients corresponded well with the previous literature that SDAVFs usually present after the fourth or fifth decade of life, with male predominance (16) and perimedullary AVFs present at age 20–40 years (17). There were no significant differences in patients' sex distribution and duration of myelopathy between the two groups.

Uneven longitudinal distributions of FVPVs were seen in 15 of 25 (60%) SDAVF (Figs. 1 and 2) or perimedullary AVF (Figs. 3 and 4) patients. In 12 of 15 (80%) patients showing uneven longitudinal distributions of FVPVs, the most crowded levels of FVPVs on MRI corresponded to the fistulous level confirmed on the spinal angiography within a ± two-level difference (Table 2, Figs. 1–4). Even longitudinal distribution of FVPVs were seen in 10 of 25

patients (40%) with SDAVFs or perimedullary AVFs. In eight of 10 (80%) patients, the true fistulous levels were located more cranial to the highest FVPVs (two of 10, 20%) or within the upper two-thirds of the FVPVs (six of 10, 60%) (Table 2). The longitudinal distribution pattern between SDAVFs and perimedullary AVFs did not show a significant difference ($P = 0.18$, Table 3).

There was a significant difference in the axial distribution pattern of FVPVs between the two types ($P < 0.01$, Table 3). While dorsal dominance was predominant in SDAVFs (13 of 18, 72%, Figs. 1 and 2), ventral dominance (Figs. 3 and 4) was major in perimedullary AVFs (five of seven, 71%).

There was no significant difference in the duration of myelopathy between the groups with and without a T2 high SI in the cord ($P = 0.20$). However, correlation analysis between the extent of the T2 high SI and the duration of myelopathy showed a significant negative correlation ($P = 0.034$, $\rho = -0.43$). There was no significant difference in the duration of myelopathy between the groups with and without enhancement in the cord ($P = 0.90$).

Perimedullary AVFs: Variceal pooling of contrast enhancement

In two of seven perimedullary AVFs, MRI revealed epidural variceal pooling of contrast enhancement: a 34-month-old female, FVPV from T9 to S2 with epidural variceal pooling at T12–L1, most crowded at T12–L1, ventral-dominant axial distribution, (Fig. 4); a 63-year-old female, FVPV from T7 to S2 with epidural variceal pooling at L2, most crowded at L2, dorsal-dominant axial distribution.

Epidural AVFs: MRI findings

All four epidural AVFs were associated with vertebral fracture. Three of four patients underwent MR examination 60–180 days after their symptoms had developed. The MRI revealed chronic compression fractures of vertebral bodies and FVPVs representing engorged veins due to long-standing AVFs. In one of the three patients, a 66-year-old female, MRI showed an engorged basivertebral vein inside the fractured L1, representing an intraosseous AVF.

However, one patient underwent MR examination 3 days after trauma. MRI showed no FVPVs but a C1 burst fracture, a comminuted C2 fracture involving bilateral lateral masses and the posterior body extending to bilateral transverse foramens, and C1/2 cord contusion. Since FVPVs were absent, a spinal AVF was not suggested on MR examination. CTA showed early venous opacification abutting the right vertebral artery (V3) adjacent to the fracture site of the C1 right posterior arch on the arterial phase, indicating an AVF, which was confirmed on spinal angiography. Spinal angiography also depicted another small fistula in the C2 body that was fed from the left V2 basivertebral artery and drained to the epidural plexus.

False positive cases on MRI (n = 3)

In three cases, although spinal vascular malformations had been suspected on spine MRI, spinal angiographies did not show evidence of spinal vascular malformations. Two of these cases showed intradural FVPVs at the lower thoracic level: a 51-year-old female, intradural serpentine enhancing FVPV from T7 to T12 level, even longitudinal distribution, dorsal-dominant axial distribution, neither T2 high SI nor enhancement at the cord; a 63-year-old male, intradural FVPV from T8 to T12 level, most crowded at T8–9 level, dorsal-dominant axial distribution, T2 high SI without enhancement at T9/10

cord. In another case, MRI of a 20-year-old male showed a subtle T2 high SI at the T3 cord, which was likely to be compressive myelopathy due to epidural lipomatosis. However, a slight prominence of the epidural veins raised suspicion of early spinal vascular malformation; this led to spinal angiography but no spinal vascular malformation was demonstrated. Retrospectively reviewing the MRI, the formerly suspected epidural veins were not likely to be suggesting vascular malformation.

Tables

Table 1. Demographics and clinical findings

	SDAVF (n = 18)	Perimedullary AVF (n = 7)	Epidural AVF with chronic vertebral fracture (n = 3)	Epidural AVF with acute vertebral fracture (n = 1)	Normal (n = 3)	Total (n = 32)
Age (year, mean ± SD)	59 ± 11	39 ± 22	63 ± 11	52	45 ± 22	53 ± 17
Sex (M:F)	14:4	5:2	2:1	1:0	2:1	24:8
Symptom						
Pure motor	3 (17%)	2 (29%)	3 (100%)	0 (0%)	2 (67%)	10 (31%)
Pure sensory	3 (17%)	3 (43%)	0 (0%)	0 (0%)	1 (33%)	7 (22%)
Pure sphinctor	0 (0%)	0 (0%)	0 (0%)	0 (0%)	0 (0%)	0 (0%)
Motor and sensory	5 (28%)	0 (0%)	0 (0%)	0 (0%)	0 (0%)	5 (16%)
Motor and sphinctor	0 (0%)	1 (14%)	0 (0%)	0 (0%)	0 (0%)	1 (3%)
Sensory and sphinctor	0 (0%)	1 (14%)	0 (0%)	0 (0%)	0 (0%)	1 (3%)
Motor, sensory, and sphinctor	6 (33%)	0 (0%)	0 (0%)	0 (0%)	0 (0%)	6 (19%)
Other symptom	0 (0%)	0 (0%)	0 (0%)	1 (100%)[a]	0 (0%)	1 (3%)

Asymptomatic	1 (6%)	0 (0%)	0 (0%)	0 (0%)	0 (0%)	1 (3%)
Mode of onset						
Acute	1 (6%)	1 (14%)	0 (0%)	1 (100%)	1 (33%)	4 (13%)
Insidious	17 (94%)	6 (86%)	3 (100%)	0 (0%)	2 (67%)	28 (88%)
Duration of symptom (day, mean ± SD)	412 ± 822	214 ± 169	110 ± 62	3	73 ± 94	296 ± 630
Treatment response						
Good	15 (83%)	4 (57%)	3 (100%)	0 (0%)	N/A	-
Fair	3 (17%)	3 (43%)	0 (0%)	1 (100%)	N/A	-
Poor	0 (0%)	0 (0%)	0 (0%)	0 (0%)	N/A	-

Note.–SDAVF = spinal dural arteriovenous fistula, AVF = arteriovenous fistula, SD = standard deviation, N/A = not applicable.

Data are number of patients with percentage in parentheses.

[a]Occipital neuralgia.

Table 2. Longitudinal distribution pattern of FVPVs and prediction of the fistulous level in SDAVFs and perimedullary AVFs

	SDAVF (n = 18)	Perimedullary AVF (n = 7)	SDAVF and perimedullary AVF (n = 25)
Longitudinal distribution pattern[a]			
Uneven	9	6	15
Accuracy of prediction[b]			
Equal	3 (33%)	2 (33%)	5 (33%)
Within ± 1 level	5 (56%)	4 (67%)	9 (60%)
Within ± 2 levels	6 (67%)	6 (100%)	12 (80%)
Even	9	1	10
Location of true fistulous level[c]			
More cranial to the highest FVPV	2 (22%)	0 (0%)	2 (20%)
Cranial 1/3 within FVPVs	3 (33%)	1 (100%)	4 (40%)
Middle 1/3 within FVPVs	2 (22%)	0 (0%)	2 (20%)
Caudal 1/3 within FVPVs	0 (0%)	0 (0%)	0 (0%)
More caudal to the lowest FVPV	2 (22%)	0 (0%)	2 (20%)
Overall longitudinal extent of FVPVs[d]			

Uneven longitudinal distribution group	10 ± 6 [5–23]	11 ± 4 [4–16]	10 ± 5 [4–23]
Even longitudianl distribution group	8 ± 5 [2–17]	12[e]	8 ± 5 [2–17]

Note.–FVPV = flow void pial vessel, SDAVF = spinal dural arteriovenous fistula, AVF = arteriovenous fistula.

[a]Data are number of patients with percentage in parentheses.

[b]Accuracy of prediction is defined as the difference between the most crowded level of FVPVs on MRI and the true fistulous level.

[c]The reference standard for the true fistulous level is the spinal angiographic finding.

[d]Data are number of vertebral segments and presented in format of mean ± SD [minimum–maximum].

[e]This is a measured value of a single case.

Table 3. Longitudinal and axial distribution patterns of FVPVs of SDAVFs and perimedullary AVFs

	SDAVF (n = 18)	Perimedullary AVF (n = 7)	*P* value[a]
Longitudinal distribution pattern			0.18
Even	9 (50%)	1 (14%)	
Uneven	9 (50%)	6 (86%)	
Axial distribution pattern			<0.01
Ventral dominance	2 (11%)	5 (71%)	
Dorsal dominance	13 (72%)	1 (14%)	
Co-dominance	3 (17%)	1 (14%)	

Note.–FVPV = flow void pial vessel, SDAVF = spinal dural arteriovenous fistula, AVF = arteriovenous fistula.

Data are number of patients with percentage in parentheses.

[a]Fisher's exact test.

Figures

Figure 1. 45-year-old male with SDAVF

A. A sagittal T2-weighted image demonstrated abnormally dilated, coiled perimedullary vessels from T4 to L5, especially on the dorsal aspect of the spinal cord. An ill-defined high SI lesion (arrow) in the spinal cord from T8 to the conus medullaris suggested cord edema from venous congestion due to spinal AVF. Considering dorsal dominancy of the dilated perimedullary vessels, SDAVF was more likely. The FVPVs were most crowded at T5–T8 (arrowhead).

B. The abnormally dilated perimedullary vessels on the dorsal aspect showed enhancement (arrowhead) on the axial T1-weighted postcontrast image.

C. The frontal view of T4 segmental arteriography showed the dural AVF at T4 with an engorged perimedullary venous structure most crowded at T5 (arrowhead). The curved arrow denotes the left T4 intercostal artery.


A.
T5
T8
L5

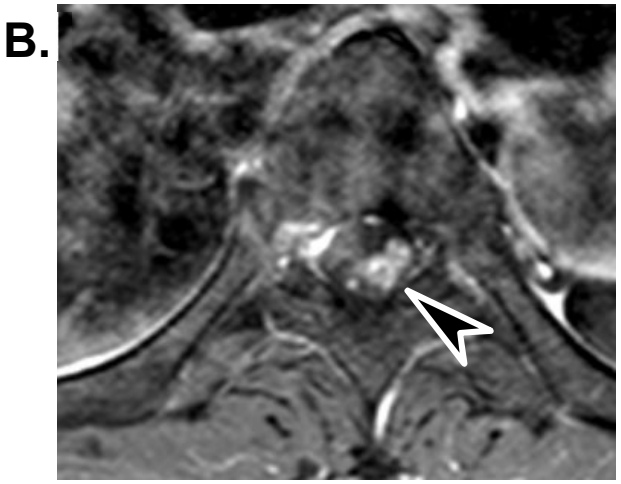
B.

C.

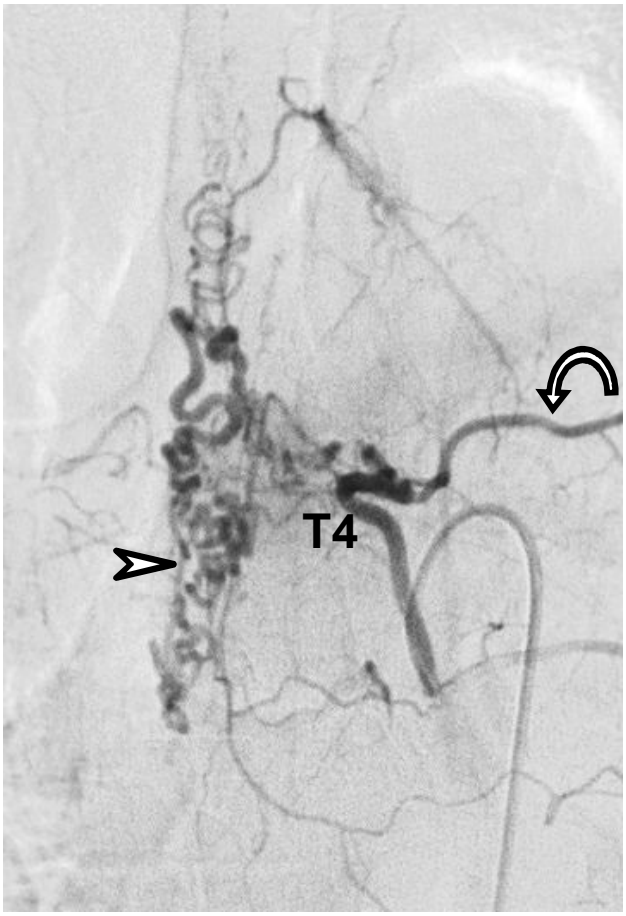

Figure 2. 70-year-old male with SDAVF

A. A sagittal T2-weighted image revealed an ill-defined high SI lesion in the T8–9 cord (arrow) as a sign of chronic venous congestion. The tortuous and dilated perimedullary vessels were present as flow voids. The combination of pathologically dilated vessels and edema of the cord led to diagnosis of spinal AVF. Dorsal location of the engorged perimedullary vessels favored SDAVF and the fistula was suspected to be located near T9/10, where the flow voids were most crowded (arrowhead).

B. A frontal projection of the right T10 intercostal arteriography confirmed the SDAVF. Please note the crowded perimedullary venous engorgement at T9–10 (arrowhead).

B.

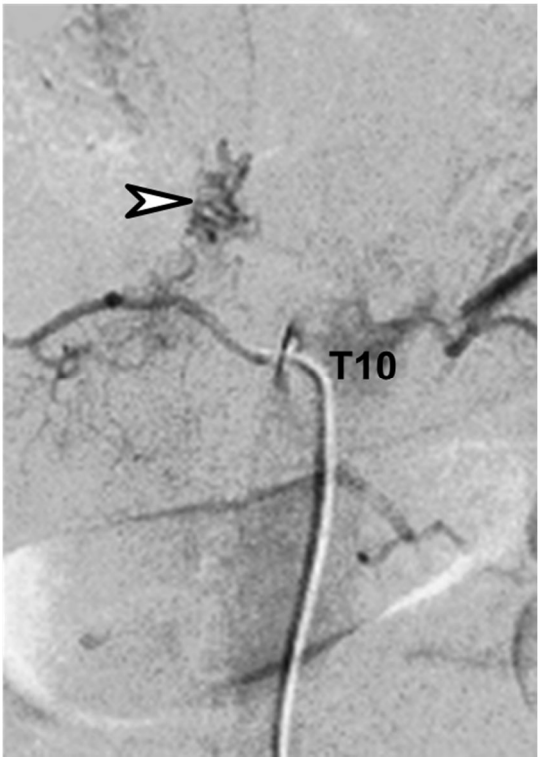

Figure 3. 43-year-old male with perimedullary AVF

A. A sagittal T2-weighted image showed an ill-defined high SI lesion in the T8–10 cord (arrow) and the tortuous and dilated perimedullary vessels from T6 to L5, suggesting spinal AVF. Ventral dominance of the engorged perimedullary vessels favored perimedullary AVF and the fistula was suspected to be located near L2–3, where the flow voids were most crowded (arrowhead). The L1 lumber arteriography (not demonstrated) revealed the anterior spinal artery being the feeder of a perimedullary AVF and the fistula formation at the level of lower portion of the L2 vertebral body.

B. On the axial T2-weighted image, dilated perimedullary vessels (arrowheads) showed enhancement, being distinguished with non-enhancing nerves.


A.
T6
L5

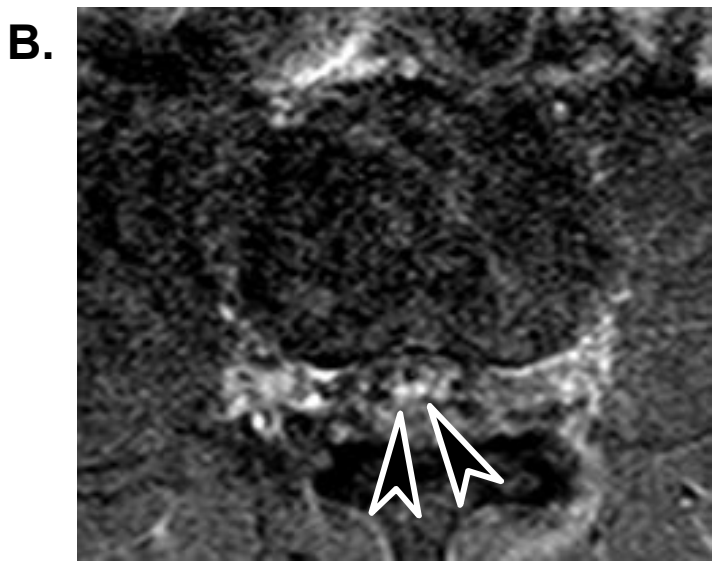
B.

Figure 4. 34-month-old female with perimedullary AVF

A. A Sagittal T2-weighted image revealed an ill-defined high SI lesion in the T5–L1 cord (arrow) and abnormally dilated, coiled perimedullary vessels from T9 to S2. A spinal AVF was predicted to be located near T12–L1, where the engorged vessels were most crowded (arrowhead).

B. A sagittal T1-weighted postcontrast image showed epidural variceal pooling at T12–L1 (asterisk).

C. Three-dimensional reconstruction of left T10 intercostal rotational arteriography depicted a perimedullary AVF at the L1 level (arrowhead) and varix formation (asterisk).

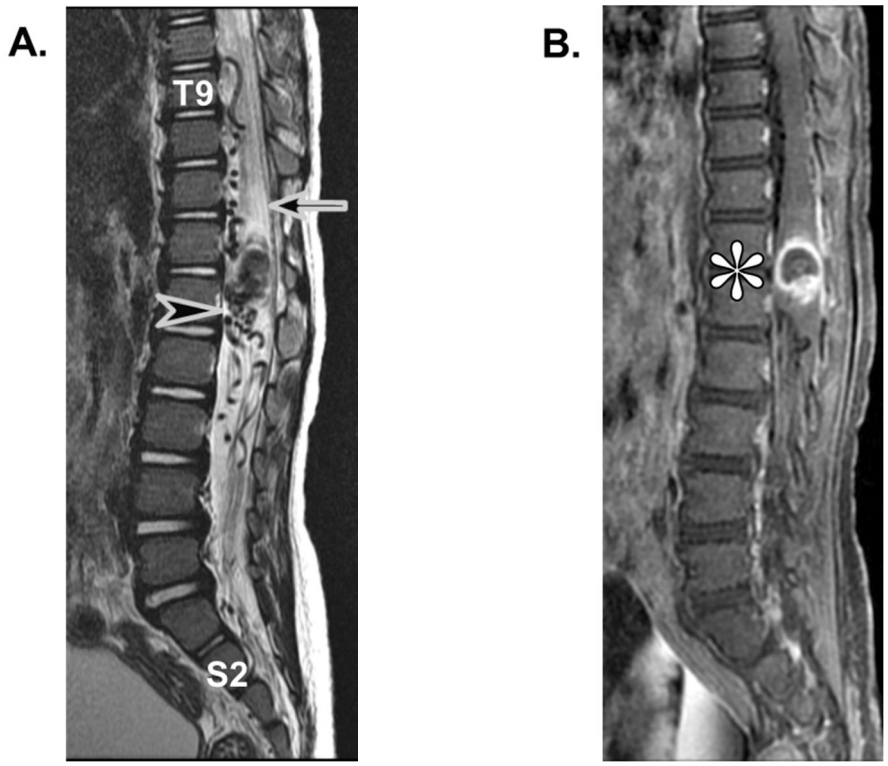

C.

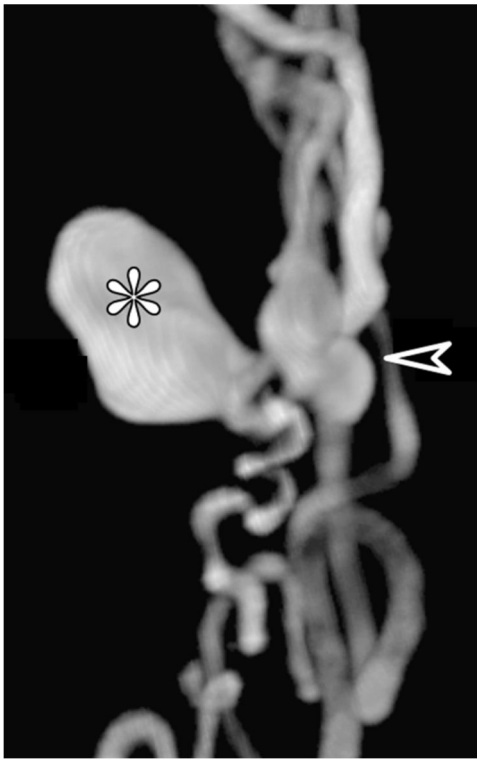

Discussion

Our results showed that detecting the most crowded level of FVPVs on MRI may help localizing the fistulous level. The search for a spinal fistula with a complete spinal angiography is often tedious and exhaustive since it may include as many as 40 selective injections (18), requires considerable time with high radiation exposures in which a large volume of potentially nephrotoxic contrast agents are administered, and is accompanied by a certain risk of neurological complication (8, 19). Fortunately, performing noninvasive modalities, such as MDCTA and CEMRA prior to conventional angiography has been reported to be a useful guide for the angiographers to reach certain spinal levels (10, 20, 21).

However, the first diagnostic imaging technique of myelopathy is often conventional MRI, not CEMRA. Our results are clinically relevant in that they suggest the added value of the conventional MRI, the primary diagnostic tool, in localizing the fistulous level and differentiating its type. In addition, CEMRA has limitation in that contrast agent has to be used and both high spatial and time resolutions are necessary for its reliability, necessitating the high-end machine. Moreover, the reliability of CEMRA is strongly dependent on the quality of postprocessing, i.e., multiplanar reconstruction, which is elaborate and time consuming and requires considerable skill and dedication (14), thereby limiting its clinical usefulness considering the acute or subacute course of spinal AVFs.

Our analysis suggests that the axial distribution pattern of FVPVs on MRI may be a differentiating feature between SDAVFs and perimedullary AVFs. It is regarded that those two entities cannot be differentiated on MRI since both may lead to congestive edema and small dilated epidural vessels

(17). Recently, Lai et al. (20) have reported two cases each, respectively diagnosed as SDAVF and perimedullary AVF, with MDCTA. However, to our knowledge there has been no report on differentiating features between SDAVFs and perimedullary AVFs on conventional MRI. An SDAVF is treated with either glue embolization or surgery (5, 17), while a perimedullary AVF type I is treated with surgery and type II and III are treated with coil or balloon embolization (17). Different management of each AVF necessitates defining its exact type, and predicting the type with preangiographic MRI may be helpful in reducing the angiography and planning subsequent treatment.

The two perimedullary AVF cases suggest that variceal pooling of contrast enhancement on MRI may be helpful in diagnosing a perimedullary AVF (Fig. 4). According to our study, there was no case of SDAVF that showed variceal pooling on MRI. This result corresponds well with the limited reporting of a varix with an SDAVF (22, 23). Theoretically, association between a varix and an SDAVF is an unexpected condition because SDAVFs are low-flow lesions (24). On the other hand, some perimedullary AVFs have a high shunt volume leading to massive remodeling of the blood vessels with markedly enlarged arteries and veins and varices (25).

Our results that all four epidural AVFs were associated with vertebral fractures correspond to the previous literature (26, 27). MRI and angiographic findings of the three patients with a chronic compression fracture strongly supported that the epidural AVFs were related to trauma: 66-year-old female, chronic compression fracture and engorged basivertebral veins at the L1 vertebral body, supplied by multiple feeders including bilateral L1, left T12, and L2 intercostal arteries; 72-year-old male, chronic compression fracture at the T12 vertebral body, SDAVF through bilateral T12 intercostal arteries, and epidural AVF through left T11 intercostal artery; 50-year-old male, chronic

compression fracture at the L2 vertebral body, epidural fistula at L2. It has been hypothesized that trauma can lead to the development of an epidural or paraspinal AVF. Several mechanisms of fistula formation have been suggested. Trauma with or without vertebral fractures results in microtears of the affected arterial wall and produces an AVF (28). It is also possible that traumatic events can cause thrombosis or thrombophlebitis of the veins. A fistula can develop due to arterial growth during the process of organization and recanalization (28, 29). Another mechanism of fistula formation is increased venous pressure due to impaired venous drainage after trauma causing spontaneous occurrence (29).

In our study, there were three false positive cases which were finally diagnosed as normal. In those cases, prominent FVPVs were seen on the dorsal surface of the lower thoracic spinal cord without any intramedullary signal change. Therefore, minimal FVPVs on the dorsal surface of the lower thoracic spinal cord could be considered as normal if there is no combined intramedullary signal change or no myelopathy.

There were two limitations to our study. First, the sample size was relatively small. However, given the low incidence of spinal vascular malformation, our sample, comprised of 29 spinal vascular malformations, is relatively large. Second, because of the retrospective nature of the study, the use of various MR machines and some degree of selection bias were inevitable.

In conclusion, fistulous levels may be predicted to be within the most crowded level of FVPVs ± two-level, and the dorsal dominance pattern of FVPVs favors SDAVFs while the ventral dominance pattern suggests perimedullary type.

References

1. Riche MC, Reizine D, Melki JP, Merland JJ. Classification of spinal cord vascular malformations. Radiation medicine. 1985;3(1):17-24.

2. Bemporad JA, Sze GS. MR imaging of spinal cord vascular malformations with an emphasis on the cervical spine. Magnetic resonance imaging clinics of North America. 2000;8(3):581-96.

3. Gilbertson JR, Miller GM, Goldman MS, Marsh WR. Spinal dural arteriovenous fistulas: MR and myelographic findings. AJNR American journal of neuroradiology. 1995;16(10):2049-57.

4. Atkinson JL, Miller GM, Krauss WE, Marsh WR, Piepgras DG, Atkinson PP, et al. Clinical and radiographic features of dural arteriovenous fistula, a treatable cause of myelopathy. Mayo Clinic proceedings. 2001;76(11):1120-30.

5. Van Dijk JM, TerBrugge KG, Willinsky RA, Farb RI, Wallace MC. Multidisciplinary management of spinal dural arteriovenous fistulas: clinical presentation and long-term follow-up in 49 patients. Stroke; a journal of cerebral circulation. 2002;33(6):1578-83.

6. Benhaiem N, Poirier J, Hurth M. Arteriovenous fistulae of the meninges draining into the spinal veins. A histological study of 28 cases. Acta Neuropathol. 1983;62(1-2):103-11.

7. Heros RC, Debrun GM, Ojemann RG, Lasjaunias PL, Naessens PJ. Direct spinal arteriovenous fistula: a new type of spinal AVM. Case report. Journal of neurosurgery. 1986;64(1):134-9.

8. Luetmer PH, Lane JI, Gilbertson JR, Bernstein MA, Huston J, 3rd, Atkinson JL. Preangiographic evaluation of spinal dural arteriovenous fistulas with elliptic centric contrast-enhanced MR Angiography and effect on radiation dose and volume of iodinated contrast material. AJNR American journal of neuroradiology. 2005;26(4):711-8.

9. Lai PH, Pan HB, Yang CF, Yeh LR, Hsu SS, Lee KW, et al. Multi-detector row computed tomography angiography in diagnosing spinal dural arteriovenous fistula: initial experience. Stroke; a journal of cerebral circulation. 2005;36(7):1562-4.

10. Zampakis P, Santosh C, Taylor W, Teasdale E. The role of non-invasive computed tomography in patients with suspected dural fistulas with spinal drainage. Neurosurgery. 2006;58(4):686-94.

11. Yamaguchi S, Nagayama T, Eguchi K, Takeda M, Arita K, Kurisu K. Accuracy and pitfalls of multidetector-row computed tomography in detecting spinal dural arteriovenous fistulas. Journal of neurosurgery Spine. 2010;12(3):243-8.

12. Farb RI, Kim JK, Willinsky RA, Montanera WJ, terBrugge K, Derbyshire JA, et al. Spinal dural arteriovenous fistula localization with a technique of first-pass gadolinium-enhanced MR angiography: initial experience. Radiology. 2002;222(3):843-50.

13. Saraf-Lavi E, Bowen BC, Quencer RM, Sklar EM, Holz A, Falcone S, et al. Detection of spinal dural arteriovenous fistulae with MR imaging and contrast-enhanced MR angiography: sensitivity, specificity, and prediction of vertebral level. AJNR American journal of neuroradiology. 2002;23(5):858-67.

14. Mull M, Nijenhuis RJ, Backes WH, Krings T, Wilmink JT, Thron A. Value and limitations of contrast-enhanced MR angiography in spinal arteriovenous malformations and dural arteriovenous fistulas. AJNR American journal of neuroradiology. 2007;28(7):1249-58.

15. Oda S, Utsunomiya D, Hirai T, Kai Y, Ohmori Y, Shigematsu Y, et al. Comparison of dynamic contrast-enhanced 3T MR and 64-row multidetector CT angiography for the localization of spinal dural arteriovenous fistulas. AJNR American journal of neuroradiology. 2014;35(2):407-12.

16. Naidich TP, Castillo M, Cha S, Raybaud C, Smirniotopoulos JG, Kollias S. Imaging of the Spine: Expert Radiology Series: Elsevier Health Sciences; 2010.

17. Krings T, Mull M, Gilsbach JM, Thron A. Spinal vascular malformations. European radiology. 2005;15(2):267-78.

18. Willinsky R, Lasjaunias P, Terbrugge K, Hurth M. Angiography in the investigation of spinal dural arteriovenous fistula. A protocol with application of the venous phase. Neuroradiology. 1990;32(2):114-6.

19. Rodesch G, Lasjaunias P. Spinal cord arteriovenous shunts: from imaging to management. European journal of radiology. 2003;46(3):221-32.

20. Lai PH, Weng MJ, Lee KW, Pan HB. Multidetector CT angiography in diagnosing type I and type IVA spinal vascular malformations. AJNR American journal of neuroradiology. 2006;27(4):813-7.

21. Si-jia G, Meng-wei Z, Xi-ping L, Yu-shen Z, Jing-hong L, Zhong-hui W, et al. The clinical application studies of CT spinal angiography with 64-detector row spiral CT in diagnosing spinal vascular malformations. European

journal of radiology. 2009;71(1):22-8.

22. Glasser R, Masson R, Mickle JP, Peters KR. Embolization of a Dural Arteriovenous Fistula of the Ventral Cervical Spinal Canal in a Nine-Year-Old Boy. Neurosurgery. 1993;33(6):1089-94.

23. Inci S, Akdemir P, Ozgen T. Spinal dural arteriovenous fistula and venous aneurysm: an unusual association. Surgical neurology. 2003;60(4):334-7; discussion 7-8.

24. Hurst RW, Kenyon LC, Lavi E, Raps EC, Marcotte P. Spinal dural arteriovenous fistula: the pathology of venous hypertensive myelopathy. Neurology. 1995;45(7):1309-13.

25. Krings T, Lasjaunias PL, Thron AK. Chaper 13. Spinal Vascular Malformations. In: Naidich TP, Castillo M, Cha S, Raybaud C, Smirniotopoulos JG, Kollias S, editors. Imaging of the Spine: Expert Radiology Series: Elsevier Health Sciences; 2010. p. 261.

26. Jin YJ, Chung SK, Kwon OK, Kim HJ. Spinal intraosseous arteriovenous fistula in the fractured vertebral body. AJNR American journal of neuroradiology. 2010;31(4):688-90.

27. Chul Suh D, Gon Choi C, Bo Sung K, Kim KK, Chul Rhim S. Spinal osseous epidural arteriovenous fistula with multiple small arterial feeders converging to a round fistular nidus as a target of venous approach. AJNR American journal of neuroradiology. 2004;25(1):69-73.

28. McCutcheon IE, Doppman JL, Oldfield EH. Microvascular anatomy of dural arteriovenous abnormalities of the spine: a microangiographic study. Journal of neurosurgery. 1996;84(2):215-20.

29. Ushikoshi S, Goto K, Uda K, Ogata N, Takeno Y. Vertebral arteriovenous fistula that developed in the same place as a previous ruptured aneurysm: a case report. Surgical neurology. 1999;51(2):168-73.

요약

척추동정맥루의 자기공명영상 소견

-동정맥루의 위치 결정과 경막동정맥루와 척추주위동정맥루 간 감별-

양현경

서울대학교 대학원

의과대학 임상의과학과

목적: 척추동정맥루의 위치와 유형을 구체화하는 자기공명영상 소견을 찾고자 한다.

방법: 2003 년 4 월부터 2013 년 4 월까지 분당서울대병원을 방문해 척추동맥루 의증으로 척추 혈관조영술을 시행한 환자들을 대상으로 하였다. 이 환자들의 척추 자기공명영상 소견 중 흐름소실 징후를 보이는 연막혈관의 분포 양상을 영상의학과 의사 두 명이 다음과 같이 분석하여 의견 일치를 이루었다. 흐름소실연막혈관의 종단 분포 양상을 균등 또는 불균등으로 분류하고, 불균등 분포일 경우 혈관이 가장 붐비는 위치를 기술하였다. 흐름소실연막혈관의 횡단

분포 양상을 등쪽 우세, 배쪽 우세 또는 공동우세로 분류하였다. 동정맥루의 위치와 유형에 대한 참조 기준으로 혈관조영술 소견을 따랐다.

결과: 32 명(남:여=24:8, 평균 연령, 53 세; 연령 범위, 2–74 세)의 환자를 분석하였다. 최종 진단은 경막동정맥루 18 명, 척추주위동정맥루 7 명, 경막외동정맥루 4 명, 정상 3 명이었다. 불균등 종단 분포 환자 15 명 중 12 명에서 흐름소실연막혈관이 가장 붐비는 위치의 ± 2 개 척추 레벨 범위에 실제 동정맥루가 위치하였다. 경막동정맥루 환자에서는 흐름소실연막혈관이 등쪽 우세 유형이 주를 이룬 반면 (13/18), 척추주위동정맥루 환자에서는 배쪽 우세 유형이 주를 이루었다 (5/7) (유의 확률< 0.01).

결론: 흐름소실연막혈관이 가장 붐비는 위치의 ± 2 개 척추 레벨 범위에 동정맥루가 위치할 것으로 추측할 수 있다. 흐름소실연막혈관의 등쪽 우세 분포는 경막동정맥루를 시사하고, 배쪽 우세 분포는 척추주위동정맥루를 시사한다.

주요어: 중추신경계 혈관기형; 척수 질환; 동정맥루; 자기공명영상; 혈관조영술

학번: 2014-22212